

## Comparing the Effect of Three Processing Methods for Modification of Filament Yarns with Inorganic Nanocomposite Filler and their Bioactivity against *Staphylococcus aureus*

Roya Dastjerdi\*, M. R. M. Mojtahedi, and A. M. Shoshtari

Textile Engineering Department, Center of Excellence in Textile, Amirkabir University of Technology (Tehran Polytechnic), Tehran, Iran

Received March 19, 2008; Revised November 18, 2008; Accepted November 18, 2008

**Abstract:** This research compared three methods for producing and processing nanocomposite polypropylene filament yarns with permanent antimicrobial efficiency. The three methods used to mix antimicrobial agents based on silver nano particles with PP were as follows: 1) mixing of PP powder and inorganic nanocomposite filler with the appropriate concentration using a twin-screw extruder and preparing granules, 2) method 1 with a single-rather than twin-screw extruder, and 3) producing the masterbatch by a twin-screw extruder and blending it with PP in the melt spinning process. All pure polypropylene samples and other combined samples had an acceptable spinnability at the spinning temperature of 240 °C and take-up speed of 2,000 m/min. After producing as-spun filament yarns by a pilot plant, melt spinning machine, the samples were drawn, textured and finally weft knitted. The physical and structural properties (e.g., linear density, tenacity, breaking elongation, initial modulus, rupture work, shrinkage and crystallinity) of the as-spun and drawn yarns with constant and variable draw ratios (the variable draw ratio was used to gain a constant breaking elongation of 50%) were investigated and compared, while DSC, SEM and FTIR techniques were used to characterize the samples. Finally, the antibacterial efficiency of the knitted samples was evaluated. The experimental results revealed that the crystallinity reduction of the as-spun yarn obtained from method 1 (5%) was more than that of method 2 (3%), while the crystallinity of the modified as-spun yarns obtained with method 3 remained unchanged compared to pure yarn. However, the drawing procedure compensated for this difference. By applying methods 2 and 3, the drawing generally improved the tenacity and modulus of the modified fibers, whereas method 1 degraded the constant draw ratio. Although the biostatic efficiency of the nanocomposite yarns was excellent with all three methods, the modified fabrics obtained from methods 1 and 2 showed a higher bioactivity.

**Keywords:** antibacterial, filament yarn, nanocomposite, method of processing, silver/TiO<sub>2</sub>.

### Introduction

Method of processing is a very important and critical variable in production of nanocomposites. It acts as an important factor on dispersion and distribution of nanoparticles, interface interaction, microstructure and properties of nanocomposites.<sup>1</sup>

A wide range of micro-organisms coexists in a natural equilibrium with human body and living environments, but a rapid and uncontrolled multiplication of microbes can seriously lead to three unpleasant effects. The first is the degradation phenomena like coloring, discoloration and deterioration of fibers. The second one is producing of unpleasant odor and the third, which is the most important

effect, is increasing of potential health risks.<sup>2,3</sup>

Conventional fibers and polymers not only do not show any resistance against micro-organisms and materials generated from their metabolism but also they are most common materials for accumulation and proliferation of micro-organisms into the surrounding environments. In fact, several factors such as suitable temperature and humidity, presence of dust, soil, spilled food and drinks stains, skin dead cells, sweat and oil secretions of skin glands, and also finishing materials on the textile surfaces can make textile as an optimal enrichment culture for a rapid multiplication of micro-organisms.<sup>3</sup>

Polypropylene fiber is one of the most widely used synthetic fibers in textile industry especially for its various application fields. In fact, some advantages of this fiber type including cheapness, lightness, high chemical strength and high absor-

\*Corresponding Author. E-mail: roya\_dastjerdi@aut.ac.ir

bency have made it suitable for many demands, such as carpets, automotive interior trim, films, packaging, cover stock, cables, napkins, wipes and so on. In particular, it is used for sanitary applications such as surgical masks, diapers, filters, hygienic bands, etc which need to display antibacterial effects.<sup>4</sup>

Silver is one of the safer antibacterial agents in comparison with some possible organic antibacterial agents that have been avoided because of the risk of their harmful effects to the human body.<sup>5,6</sup> Silver has been described as being 'oligodynamic' because of its ability to exert a bactericidal effect on products containing silver, principally due to its antimicrobial activities and low toxicity to human cells.<sup>2,6</sup> Its therapeutic property has been proven against a broad range of micro-organisms (over 650 disease-causing organisms in the body) even at low concentrations.<sup>7,8</sup> Silver nanoparticles are a non-toxic and non-tolerant disinfectant.<sup>9</sup> Using silver nanoparticles leads to increasing the number of particles per unit area and thus antibacterial effects can be maximized.<sup>4</sup>

TiO<sub>2</sub> nanoparticles have unique properties (e.g. stable, long lasting, safe and broad-spectrum antibiotics).<sup>7,10</sup> Irradiation of anatase titanium dioxide by light with energy more than its band gaps generates electron-hole pairs that induce redox reactions at the surface of the titanium dioxide. Consequently, electrons in TiO<sub>2</sub> jump from the valence band to the conduction band, and the electron ( $e^-$ ) and electric hole pairs ( $h^+$ ) form on the surface of the photocatalyst. The created negative electrons and oxygen will combine into O<sub>2</sub><sup>-</sup>, the positive electric holes and water will generate hydroxyl radicals. Ultimately, the produced various highly active oxygen species can oxidize organic compounds of cell to carbon dioxide (CO<sub>2</sub>) and water (H<sub>2</sub>O). Thus titanium dioxide can decompose common organic matters in the air such as odour molecules, bacteria and viruses.<sup>11,12</sup> Moreover, many investigations confirm addition of noble metals such as gold and silver (as well as what used in this research) increases the

photocatalytic efficiency of titanium dioxide.<sup>11</sup> In addition, surface coating of nano-silver on titanium dioxide maximizes the number of particle per unit area in surface in comparison with using equal mass fraction of pure silver (Figure 1).

This research has been started from the modification of polymer powder as a common by-product of petrochemical companies. The processability of these starting materials prepared by three different methods and the characteristics of produced samples (fiber to fabric) have been investigated. Finally, the microbiological efficiency of the produced fabric has been further studied.

## Experimental

**Materials.** Isotactic polypropylene powder, supplied by Navidzarchimie petrochemical company, Iran, was used as a polymer matrix for preparation of pure and modified granules in method 1 and 2 and preparation of modified masterbatch in method 3.

Isotactic polypropylene granule (SABIC PP 512 MN10), supplied by Sabic, Saudi Arabia, was used for mixing with prepared masterbatch during melt spinning process in method 3. The melt flow index (MFI) of this granule has been recorded in Table I.

The filler, Nanocid P101, kindly provided by Pars Nano Nasb Research department of Iran Nasb Niroo Co, Iran, is a nanocomposite of anatase TiO<sub>2</sub> as the carrier core coated with 1% wt of nano-silver particles. TiO<sub>2</sub> nanoparticles have a wide range of size under 80 nm and are covered imperfectly by thin films of silver having the thickness under 30 nm as stated by supplier.

**Method.** Three methods were used for preparation of polypropylene nanocomposite filament yarns.

**Method 1: Modification of Granule by Means of Twin Screw Extruder:** The development of bacteriostatic nanocomposite filament yarn has been realized in two stages:

In the first stage, the powder materials PP and antibacterial agent were premixed and melt blended in a co-rotating-screw extruder (Brabender, Germany). Pure PP granule and nanocomposite granules containing silver/TiO<sub>2</sub> nanocomposite were prepared. The melt flow index (MFI) of pure and modified granules has been recorded in Table I.

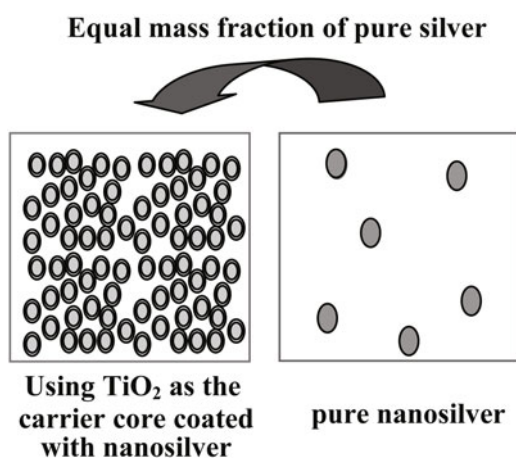


**Figure 1.** Increasing the available nanosilver particles via surface coating of nanosilver on titanium dioxide.

**Table I. MFI of the Pure PP, Modified Masterbatch and Granules**

Method	Sample	Melt Flow Index (g/10 min)
1	Prepared granule of pure PP	26.20
	Prepared modified granule	24.80
2	Prepared granule of pure PP	24.80
	Prepared modified granule	22.10
3	Pure PP granule	22.90
	Modified masterbatch	28.10

In the second stage, pure PP fiber and the composite fibers containing nano-filler were prepared by an Automatik pilot plant spinning machine (Germany). This machine has an extruder using two spinning nozzles. Two 36 holes spinnerets of 0.25 mm hole diameter were used for spinning partially oriented filament yarns at the spinning temperature of 240 °C and the take up speeds of 2,000 m.min<sup>-1</sup>.<sup>13</sup>

**Method 2: Modification of Granule by Means of Single Screw Extruder:** Similar to method 1, but in the first stage, pure and modified granule prepared using a single screw extruder (Colline, Germany). Melt flow index (MFI) of these granules has been recorded in Table I.

**Method 3: Preparation of Masterbatch:** In the first stage, polypropylene (iPP) powder and the silver/TiO<sub>2</sub> nanocomposite were premixed and melt blended in the twin screw extruder at the same conditions used in granule modification. The melt flow index (MFI) of the prepared masterbatch has been recorded in Table I.

In the second stage, melt spinning was carried out from mixing of virgin PP granule and the master-batch obtained in the first stage at the same spinning conditions used in method 1.<sup>14</sup> The inorganic filler used in the three methods was the same.

**Drawing:** Drawn samples have been prepared with a Zinser D5203 drawing machine (Germany) using two different methods.

1. The constant draw ratio ( $\lambda = 2.5$ ).
2. The variable draw ratio was used to gain the constant breaking elongation of 50% under the same conditions of 1. The above breaking elongation was selected for having a suitable further texturing process.

**Texturing:** For all samples a Scragg-Shirley minibulk false-twist texturing machine (England) was applied at the heater temperature of 150 °C, draw ratio of 1.07, texturing speed of 100 m.min<sup>-1</sup>, spindle speed of 300,000 rpm and applied twist of 2,953 rpm. Textured yarns were finally weft knitted.

**Test Methods. Density-Based Crystallinity (Structural Analysis):** Density of nanocomposite yarns ( $\rho_i$ ) has been measured according to ASTM D792 using mixture of distilled water and ethanol.

First, The density of matrix ( $\rho_{pp}$ ) was calculated from eq. (1).<sup>15</sup>

$$1/\rho_i = w_f/\rho_f + w_{pp}/\rho_{pp} \quad (1)$$

Where  $\rho_f$  is the density of nanocomposite filler,  $w_f$  and  $w_{pp}$  are weight fractions of nanocomposite filler and PP, respectively,

$\rho_f = 3.86 \text{ g/cm}^3$  was obtained from substituting  $\rho_{silver} = 10.5 \text{ g/cm}^3$  and  $\rho_{TiO_2} = 3.84 \text{ g/cm}^3$  in eq. (2).<sup>16</sup>

$$1/\rho_f = w_{silver}/\rho_{silver} + w_{TiO_2}/\rho_{TiO_2} \quad (2)$$

Where  $w_{TiO_2}$  and  $w_{silver}$  are weight fractions of titanium diox-

ide and silver, respectively.

Finally density-based crystallinity ( $X_c$ ) was calculated from eq. (3).

$$X_c = \left( \frac{\rho_{pp} - \rho_a}{\rho_c - \rho_a} \right) \frac{\rho_c}{\rho_{pp}} \times 100 \quad (3)$$

Where  $\rho_a = 0.8576 \text{ g.cm}^{-3}$  and  $\rho_c = 0.9363 \text{ g.cm}^{-3}$  are the density of amorphous and crystalline areas.<sup>17</sup>

**Differential Scanning Calorimetry (DSC):** Thermal properties were studied employing a TA Instrument Differential Scanning Calorimetry 2010 (U.S.A) at the heating rate of 5 °C/min. Crystallinity of studied samples was also calculated using the following equation.

$$X = \left( \frac{\Delta H}{(1-w_f)\Delta H^*} \right) \times 100 \quad (4)$$

$w_f$  is weight fractions of nanocomposite filler,  $\Delta H$  refers to the measured melting enthalpy and  $\Delta H^*$  denotes 100% crystalline polypropylene that equals 209 J.g<sup>-1</sup>.<sup>18</sup>

**FTIR Spectroscopy:** The influence of silver/anatase TiO<sub>2</sub> nanocomposite on PP thermal degradation during melt spinning was investigated using a Nicolet FTIR instrument by taking the wavelengths from 400 to 4000 cm<sup>-1</sup> at the ambient temperature. Following the work of Aslanzadeh and Haghghat Kish,<sup>19</sup> Rabello and White,<sup>20</sup> Castejon *et al.*<sup>21</sup> and Carlsson *et al.*,<sup>22</sup> the unaffected peak by degradation at 2720 cm<sup>-1</sup> was taken as the reference for normalizing the peaks (by dividing each absorbed intensity to the intensity at 2720 cm<sup>-1</sup>).

**Linear Density:** The linear density of yarns was determined as an average of 5 measurements of the weight of 100 m of yarns.

**Evaluation of Antibacterial Efficiency:** Antibacterial efficiency was expressed according to AATCC 100 that is formulated as:

$$R(\%) = \frac{A-B}{A} \times 100 \quad (5)$$

Where  $A$  is the number of bacteria recovered from the inoculated test specimen swatches in the jar after 24 h incubation with unmodified fiber and  $B$  is the number of bacteria according to "A" conditions, but with antibacterial modified fiber. Consequently  $R(\%)$  is the percentage reduction ratio which indicates biostatic efficiency.

**Morphological Properties:** The SEM micrographs were obtained by means of a Vega ©Tescan scanning electron microscopy applying 20 KeV acceleration voltage to gain approximately 30,000-47,000 magnification.

**Rheological Measurements:** Melt-flow index was recorded as the mass (grams) of molten polymer passing through a fixed capillary under the constant pressure (2.16 kg) at 230 °C for 10 min (according to ASTM D1238).

**Tensile Properties:** Tensile properties were evaluated by an EMT 3050 tensile tester (Iran). The conditions of measurements were as follows: gauge length of 100 mm for as-

spun yarns, and 300 mm for drawn yarns, and deformation rate of 500 mm.min<sup>-1</sup> (according to ASTM (D3822-95a)). Average values obtained from measurements of 10 samples.

**Shrinkage:** The shrinkage of as-spun and drawn samples was measured after heating for 10 min at 130 °C according to DIN 53840.

**Results and Discussion**

The effect of filler on the crystallinity of fibers has been summarized in Table II. Adding the antimicrobial agent by applying method 1 resulted in the reduction of crystallinity up to 5%. This reduction was lower in method 2. However, by applying method 3, crystallinity of as-spun yarns remained unchanged compared to the pure PP yarn (Figure 2). It may refer to the higher increasing of particle dispersion in method 1 and 2 specially during mixing by the twin screw extruder in method 1. After drawing, the change of crystal-

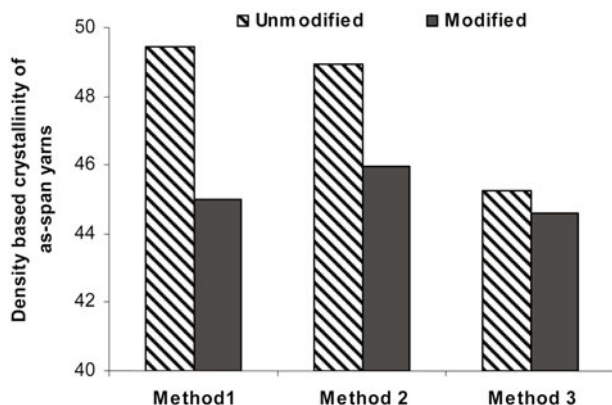


Figure 2. Density based crystallinity of as-span filament yarns.

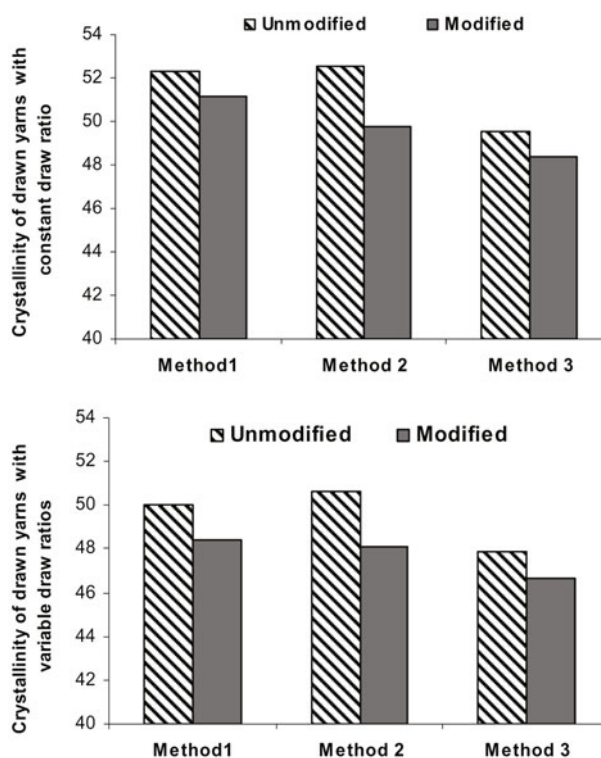


Figure 3. Density based crystallinity of drawn yarns.

linity was not substantial (Figure 3). It seems that drawing procedure has compensated this difference. The drawing led to decreasing the linear density of filaments. This reduction has resulted in compensating the effect of heat transfer rate difference between pure and modified fibers in method 1. However, dispersion improvement during drawing can cause an inverse result in method 3.

Table II. Crystallinity, Shrinkage and Linear Density of As-span and Drawn Yarns

Method	Property	Sample Type	As-spun		Drawn V.D.R <sup>a</sup>		Drawn C.D.R <sup>a</sup>	
			Pure	Modified	Pure	Modified	Pure	Modified
1	Crystallinity wt(%)		49.43	44.98	52.27	51.16	50.06	48.42
	Shrinkage (%)		2.38	2.98	4.63	4.40	4.77	5.96
	Linear Density (Tex)		13.32	14.32	6.34	6.29	8.21	7.85
	Draw Ratio		-	-	2.5	2.5	1.922	2.016
2	Crystallinity wt(%)		48.96	45.96	52.54	49.79	50.61	48.14
	Shrinkage		2.95	3.28	4.29	4.48	5.40	5.41
	Linear Density (Tex)		14.38	13.91	6.27	6.25	7.79	8.07
	Draw Ratio		-	-	2.5	2.5	1.98	1.94
3	Crystallinity wt(%)		45.23	44.60	49.56	48.42	47.86	46.62
	Shrinkage (%)		2.11	1.86	4.49	4.29	4.41	4.53
	Linear Density (Tex)		14.37	14.46	6.22	6.26	8.21	8.50
	Draw Ratio		-	-	2.5	2.5	1.905	1.849

<sup>a</sup>C. D. R and V. D. R Indicate drawn yarns with constant draw ratio and variable draw ratio respectively.

In fact, there are several factors that affect the crystallinity, some of them decrease crystallinity, while others can increase and compensate the reduction in crystallinity. First, silver nano particles have a high thermal conductivity compared to PP as a non-polar polymeric matrix. Therefore, these particles can accelerate quenching rate of nanocomposite fiber. This acceleration results in the shorter available time at the temperature in which maximum velocity of crystal growth can take place. Consequently, the opportunity of crystal growth for PP matrix is limited. Second, the silver may sometimes be a function of nucleating agent (because nanoparticles act as a type of impurities in the PP matrix) which can cause the temperature of maximum crystallization rate to be increased. Fast passing this point can reduce crystal growth. These effects could cause such the reduction of crystallinity. On the other hand, nucleation effect during the crystallization process of PP accelerates crystallization of PP matrix. However, increasing of agglomeration decreases the effect of particles on heat transfer rate. Because, agglomeration leads to decrease the specific surface of the particles and also increase their migration to surface.

Due to these contradictory effects or because of low concentration of active filler, the crystallinity of as-spun PP fiber including nanoparticles produced by applying method 3 has remained unchanged. The maximum reduction of crystallinity of as-spun yarns by applying method 1 may refer to the increasing of particle dispersion during mixing by the twin screw extruder compared to method 2, and mixing in the lower concentration of filler compared to method 3.

After drawing, because of decreasing the linear density of filaments, the effect of heat transfer rate difference between pure and modified yarn is compensated compared to similar as-spun nanocomposite filament yarn. This phenomenon has resulted in compensating the effect of heat transfer rate difference between pure and modified drawn yarns in method 1. However, dispersion improvement during drawing can cause an inverse result in method 3. Therefore it was seen poor relationship between the crystallinity changes of drawn yarns in three aforementioned methods.

The measured crystallinity of as-spun yarns based on DSC method did not show the strictly same trend as the

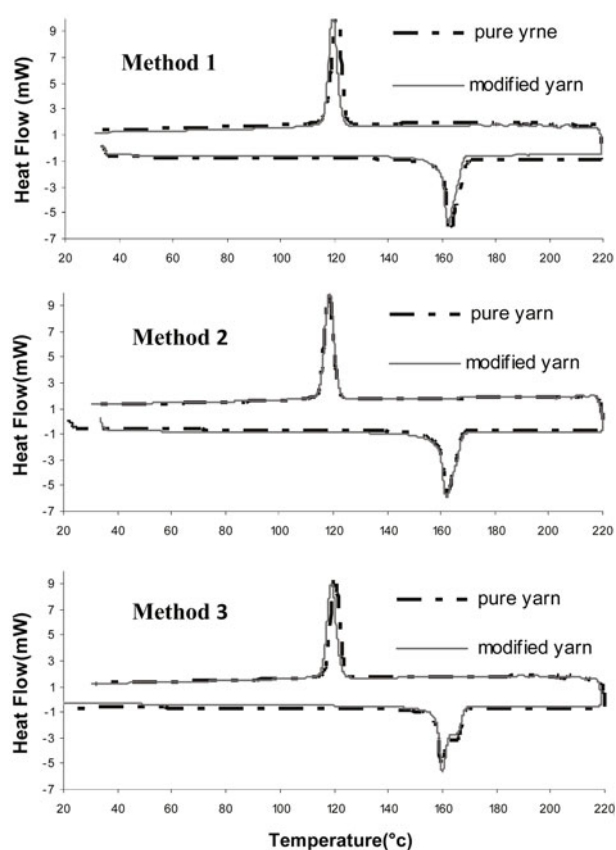


Figure 4. DSC diagram of as-spun yarns.

density based crystallinity (Table III and Figure 4). However results of density based crystallinity accompanied by more assurance because this method has more accuracy than DSC method for measurement of crystallinity. In method 1 when  $\Delta H_c$  was used for crystallinity evaluation, this reduction was higher. The evaluation of crystallinity based on  $\Delta H_c$  is independent of polymer history. Consequently, crystallinity reduction of composite fiber can be related to spatial resistance of particles against crystal growth. However, spin line tension may compensate the effect of spatial resistance of particles. Thus reduction of crystallinity based on  $\Delta H_m$  was lower. However by applying method 2 and 3 this effect was not

Table III. Thermal and Structural Properties of As-spun Yarns Obtained from DSC Method

Sample Type	Melting Temperature (°C)	Crystallization Temperature (°C)	Melting Enthalpy (J/g)	Crystallization Enthalpy (J/g)	Crystallinity(%) ( $X_{Tc}$ ) <sup>a</sup>	Crystallinity(%) ( $X_{Tm}$ ) <sup>b</sup>	
Method 1	Pure	163.2	121.0	88.94	107.1	51.24	42.56
	Modified	162.5	119.5	85.02	97.26	46.77	40.88
Method 2	Pure	162.3	118.5	85.82	96.90	46.36	41.06
	Modified	162.1	118.6	87.38	97.05	46.67	42.02
Method 3	Pure	159.8	120.4	92.66	99.58	47.65	44.33
	Modified	160.0	119.0	86.41	94.83	45.60	41.55

<sup>a</sup> $X_{Tc}$  indicates the crystallinity evaluated by Crystallization enthalpy. <sup>b</sup> $X_{Tm}$  indicates the crystallinity evaluated by Melting enthalpy.

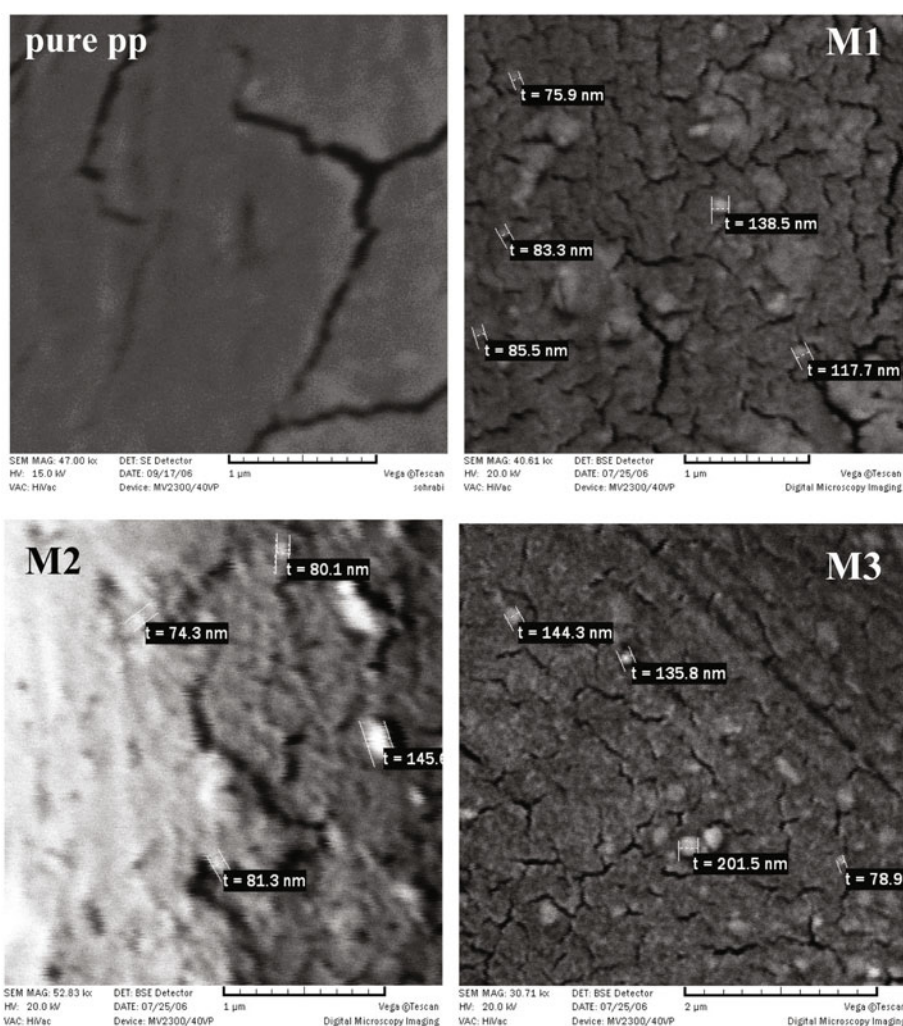


**Figure 5.** SEM micrograph of drawn yarn surface with constant draw ratio. M1, M2 and M3 indicate modified yarns by applying method 1, 2 and 3, respectively.

observed, because some possible agglomeration could decline the specific surface and space resistance of particles against the orientation of polymer chains.

SEM was carried out to observe particle dispersion on the nanocomposite filament yarns. The SEM observation showed the nanoparticles had relatively good dispersibility in method 1 and 3 (Figure 5). However, some agglomeration was observed in samples obtained by method 2.

As it was expected, the changes of shrinkage were corresponded inversely to the changes of crystallinity. Therefore as-spun yarn modified by the method 1 has the most shrinkage and after drawing the changes of shrinkage were negligible (see Table II). The changes of mechanical properties of as-spun fibers were not substantial in all three methods. Only breaking elongation changes corresponded inversely to the crystallinity variation in method 1 (see Table IV).

For investigating the effect of silver/anatase  $\text{TiO}_2$  nanocomposite on PP degradation, FTIR was used. This possible

degradation may be originated from generating active oxygen by catalytic activation of Ag. Generally this phenomenon can be led to two inverse effects on tenacity: The first is reduction of molecular weight which can decrease tenacity and the second is obtaining a narrower PDI (polydispersity index) which can increase tenacity. On the other hand, degradation phenomenon in back-bone of chain (C-C bond) can cause two other possible effects. First, generation of free radicals that can migrate to the surface during usage in form of cloths and display some health risks for people. Second, generated free radicals can act as active sites for attachment of nanoparticles to polymer and enhance compatibility. The ideal condition occurs when free radicals are generated on the branch of chain (C-H or C-C bond). Consequently the increasing of compatibility would be obtained without any risk of health care. However, the FTIR observation did not show noticeable influence of silver/anatase  $\text{TiO}_2$  nanocomposite on PP degradation (Figure 6).

**Table IV. Tensile Properties of Samples**

Properties	Sample Type	As-spun Yarns	Drawn Yarns		
			Constant Draw Ratio	Variable Draw Ratio	
Tenacity ( <i>cN/Tex</i> )	Method 1	Unmodified	12.01 (6.06)	31.01 (4.22)	22.45 (2.55)
		Modified	12.53 (4.13)	28.66 (1.31)	23.05 (3.16)
	Method 2	Unmodified	12.90 (2.98)	27.74 (5.30)	30.34 (6.96)
		Modified	12.73 (2.11)	29.06 (6.64)	29.28 (4.67)
	Method 3	Unmodified	17.57 (6.11)	39.94 (9.66)	28.40 (2.78)
		Modified	18.42 (6.74)	44.59 (7.59)	30.31 (5.79)
Initial Modulus ( <i>cN/Tex</i> )	Method 1	Unmodified	84.31 (13.37)	294.50 (4.07)	204.50 (4.15)
		Modified	89.51 (11.91)	274.10 (4.19)	221.60 (3.87)
	Method 2	Unmodified	86.94 (12.54)	256.8 (4.15)	194.5 (4.19)
		Modified	84.51 (9.02)	275.8 (3.80)	197.1 (3.93)
	Method 3	Unmodified	82.35 (9.58)	387.9 (5.69)	223.8 (3.21)
		Modified	87.35 (7.07)	430.0 (4.69)	239.5 (5.12)
Breaking Elongation(%)	Method 1	Unmodified	383.00 (3.73)	29.74 (16.71)	48.96 (32.62)
		Modified	393.50 (4.94)	32.07 (7.62)	45.74 (22.30)
	Method 2	Unmodified	369.70 (6.41)	28.42 (16.41)	52.09 (40.24)
		Modified	360.9 (5.96)	27.85 (17.67)	53.80 (29.52)
	Method 3	Unmodified	243.4 (5.74)	17.72 (16.04)	50.57 (19.12)
		Modified	217.8 (6.77)	16.96 (12.00)	53.47 (18.34)
Rupture Work	Method 1	Unmodified	34.92 (7.07)	6.34 (23.48)	8.47 (39.02)
		Modified	37.78 (6.63)	6.48 (13.39)	8.13 (26.29)
	Method 2	Unmodified	35.32 (8.25)	5.37 (23.51)	11.74 (21.01)
		Modified	33.93 (6.38)	5.49 (27.21)	12.28 (36.99)
	Method 3	Unmodified	29.68 (10.36)	4.23 (26.61)	11.25 (22.05)
		Modified	27.83 (9.59)	4.46 (21.34)	12.96 (25.20)

Values inside brackets indicate CV%.

The influence of the draw ratio on breaking elongation and rupture work is summarized in Table IV. Neither the breaking elongation nor the rupture work had significant change in all three methods.

By applying method 3, generally the drawing has improved the increase of tenacity and modulus of modified fibers, whereas in method 1 the inverse observation was noticed in the case of constant draw ratio (Figure 7). In method 2, the drawing with variable draw ratio did not show any substantial effect on the tensile strength. Only after drawing with constant draw ratio, the tensile properties increased slightly.

In other words, in method 3, the tenacity and modulus of modified fibers has improved by applying variable draw ratio. With applying higher draw ratio (drawing with constant draw ratio) this effect has enhanced in method 2 and 3. Probably, the drawing has increased the particle dispersion and improved tensile properties. Increasing modulus and tenacity can be

justified with the mechanism of energy dissipation via voiding, dewetting phenomena, chain slippage, increasing the length of crack path (zig-zag route) in polymer/filler composite, etc.<sup>23</sup> In method 1, after drawing with variable draw ratio, the intensity improvement of tensile properties in modified samples was more significant than pure sample. While the constant draw ratio, which was higher than the variable one, had an adverse result (Figure 7). Probably, the increasing of particle dispersion during mixing by the twin extruder and spinning processes had been so large that the higher draw ratio could not improve the dispersion. On the other hand, spatial resistance of particles against chain orientation has had more effect on the tensile properties. The reduction of crystal size intensified by both the quenching rate acceleration and nucleation effect of particles may also lead to this adverse effect.

However the changes of tensile properties after applying

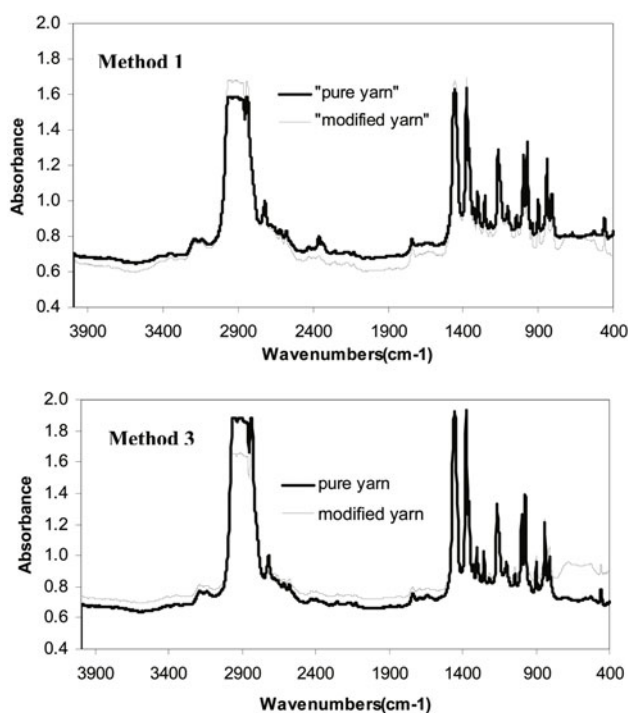


Figure 6. FTIR diagram of as-spun yarns.<sup>14</sup>

variable draw ratio (industrially more common) in all three methods were lower than 10%.

According to this viewpoint that polymer used for matrix of fibers was different in aforementioned methods, only the change percentage of properties of modified samples compared to similar unmodified sample has been considered in each method.

The antibacterial activity of silver/TiO<sub>2</sub> nanocomposite in fabric was evaluated after the specific contact time and calculated by reduction percent of *Staphylococcus aureus* ATCC 25923. The *Staphylococcus aureus* is a pathogenic microorganism that causes many diseases (e.g. toxic shock, purulence, abscess, fibrin coagulation, endocarditis). Moreover it is resistant to common antimicrobial agents.<sup>2,24</sup> Almost all tests for evaluation of textile antibacterial effectiveness have proposed testing this bacterium. Also it has been deduced that antibacterial efficiency of silver composite against *Klebsiella pneumoniae* and *Escherichia coli* is higher than *Staphylococcus aureus*.<sup>25</sup> Thus the *Staphylococcus aureus* was selected for evaluation of antibacterial efficiency in this research.

Figure 8 shows that samples had been attacked by the huge bacteria mass, during antibacterial test. However, the modified fabrics showed still a high percentage of biostatic efficiency (more than 99%) (Table V). Although the biostatic efficiency of nanocomposite fibers was excellent by applying all methods, modified fabrics obtained from method 3 showed the lowest bioactivity (Figure 9 and Table V). It can be related to the lower molecular weight of PP matrix in method 1 and

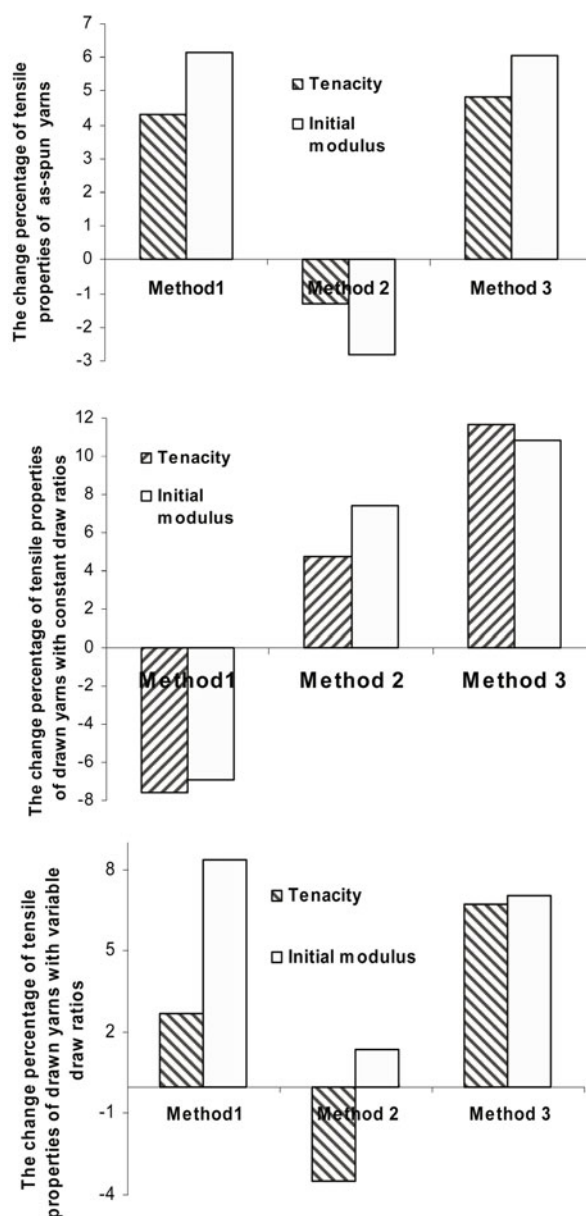


Figure 7. The change percentage of tensile properties of samples compared to the pure yarns.

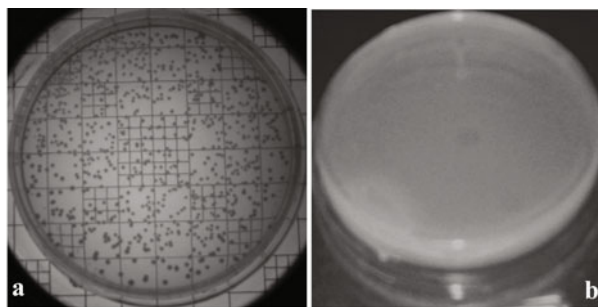
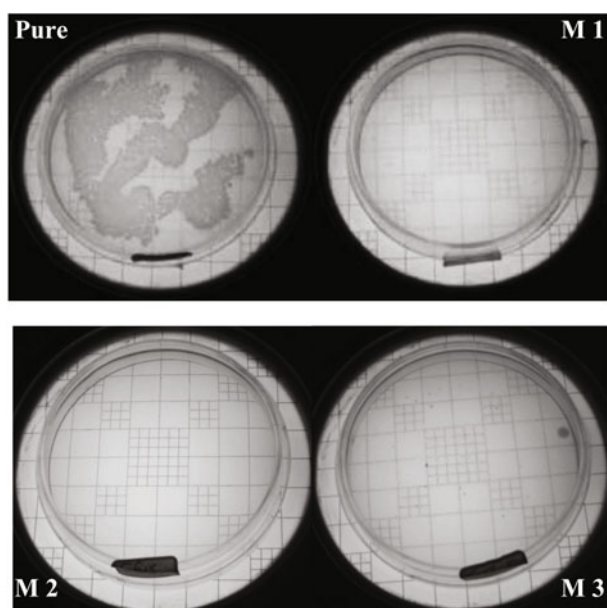


Figure 8. The mass of bacteria recovered from the inoculated pure fabric, (a) immediately after inoculation and (b) after the 24 h incubation.



**Table V. Antibacterial Efficiency of Fabric Samples**

Method	Number of Bacteria in 1 mL.10 <sup>-3</sup>	Percentage of Biostatic Efficiency
1	5.5	99.95
2	4.89	99.97
3	48.4	99.57



**Figure 9.** The designed qualitative test for evaluation of antibacterial efficiency, M1, M2 and M3 indicate modified yarns by applying method 1, 2 and 3, respectively.

2 compared to methods 3 in which higher molecular weight can reduce the release rate of particles from matrix to surface. Because of the more dispersion improvement during mixing by the twin extruder in method 1 compared to method 2, more increase in antibacterial activity was predicted with using method 1 compared to method 2. It can be concluded that although by applying method 2 some possible agglomeration can decline the specific surface of the particles and their bioactivity, increasing migration of particles to surface could compensate this reduction of bioactivity with increasing surface concentration.

Consequently, the required antibacterial performance of PP fibers was achieved by applying all three used methods. From the application point of view, it is particularly important that sufficient antibacterial effect can be attained at relatively low concentrations of filler.

## Conclusions

In this research, three various methods for investigation of possibility of producing and processing nanocomposite polypropylene filament yarns has been compared. In fact,

this research has been started from the modification of polymer powder as a by-product of petrochemical companies. The processability of these starting materials and the characteristics of produced samples (fiber to fabric) have been investigated. Finally, the microbiological efficiency of the produced fabric has been further studied.

The experimental results indicated that all samples had acceptable spinnability on the pilot plant melt spinning process. Adding the antimicrobial agent by applying method 1 and 2 resulted in the reduction of crystallinity up to 5% and 3% respectively. However, by applying method 3, crystallinity of as-spun yarns remained unchanged. Drawing procedure has compensated this difference. By applying method 2, the tensile properties improved slightly after drawing with constant draw ratio. The drawing has improved the increase of tenacity and modulus of modified fibers in method 3. While in method 1 the inverse observation was noticed in the case of constant draw ratio which had higher draw ratio than the variable one.

Although none of the applied samples displayed any bacteriocide efficiency, the biostatic efficacy of nanocomposite fibers was excellent. The sufficient bioactivity was achieved by applying all methods. Nevertheless, modified fabrics obtained from methods 1 and 2 showed the better bioactivity.

**Acknowledgments.** The authors would like to thank to Dr. Goudarzi and Mr. Moayyed at the Shahid Beheshti University of Medical Sciences & Health Services (Microbiological group) and the Iran Nasb Niroo Co.

## References

- (1) M. Pulickel, M. Ajayan, L. S. Schadler, and P. V. Braun, *Nanocomposite Science and Technology*, Wiley-VCH, Weinheim, 2003, Ch.2, p. 238.
- (2) J. V. Edwards and T. Vigo, *Bioactive Fibers & Polymers*, American Chemical Society, Washington DC, 2001.
- (3) [http://www.montefibre.it/en/polyester/pdf/sani\\_con00.pdf](http://www.montefibre.it/en/polyester/pdf/sani_con00.pdf) (accessed April 2008).
- (4) S. Y. Yeo and S. H. Jeong, *Polym. Int.*, **52**, 1053 (2003).
- (5) J. Cha, W. B. Lee, C. R. Park, Y. W. Cho, C. H. Ahn, and I. C. Kwon, *Macromol. Res.*, **14**, 573 (2006).
- (6) S. L. Percival, P. G. Bowler, and D. Russell, *J. Hosp. Infect.*, **60**, 1 (2005).
- (7) Q. Cheng, C. Li, V. Pavlinek, P. Saha, and H. Wang, *Appl. Surf. Sci.*, **252**, 4154 (2006).
- (8) S. H. Jeong, S. Y. Yeo, and S. C. Yi, *J. Mater. Sci.*, **40**, 5407 (2005).
- (9) S. H. Jeong, Y. H. Hwang, and S. C. Yi, *J. Mater. Sci.*, **40**, 5413 (2005).
- (10) Y. J. Kwark, J. Kim, and B. M. Novak, *Macromol. Res.*, **15**, 31 (2007).
- (11) G. Fu, P. S. Vary, and C. T. Lin, *J. Phys. Chem. B*, **109**, 8889 (2005).
- (12) Y. W. H. Wong, C. W. M. Yuen, M. Y. S. Leung, S. K. A. Ku,

- and H. L. I. Lam, *Autex Research Journal*, **6**, 1 (2006).
- (13) R. Dastjerdi, M. R. M. Mojtahedi, A. M. Shoshtari, and A. Khosroshahi, *J. Text. Instit.*, in press (2008).
- (14) R. Dastjerdi, M. R. M. Mojtahedi, and A. M. Shoshtari, *Macromol. Symp.*, in press (2008).
- (15) V. B. Gupta and Y. C. Bhuvanesh, *J. Appl. Polym. Sci.*, **60**, 1951 (1996).
- (16) CRC, *Handbook of Chemistry and Physics*, 52nd Edition, P:1971-1972 PB-134 and B149.
- (17) L. Mandelkern and R. G. Alamo, *Physical Properties of Polymers*, Air Press, Woodbury, New York, 1996.
- (18) W. G. F. Sengers, O. van den Berg, M. Wubbenhorst, A. D. Gotsis, and S. J. Picken, *Polymer*, **46**, 6064 (2005).
- (19) S. Aslanzadeh and M. Haghighat Kish, *Polym. Degrad. Stabil.*, **90**, 461 (2005).
- (20) M. S. Rabello and J. R. White, *Polym. Degrad. Stabil.*, **56**, 55 (1997).
- (21) M. L. Castejon, P. Tiemblo, and J. M. Gomez-Eivira, *Polym. Degrad. Stabil.*, **70**, 357 (2000).
- (22) D. J. Carlsson, F. R. S. Clark, and D. M. Wiles, *Text. Res. J.*, **46**, 590 (1976).
- (23) K. G. Gatos, N. S. Sawanis, A. A. Apostolov, R. Thomann, and J. K. Kocsis, *Macromol. Mater. Eng.*, **289**, 1079 (2004).
- (24) M. Montazer and M. G. Afjeh, *J. Appl. Polym. Sci.*, **103**, 178 (2007).
- (25) A. Marcincin, A. Ujhelyiova, J. Legen, V. Kabatova, and P. Jambrich, *Vlakana-a-textil*, **4**, 38 (1997).